Journal of Solid State Chemistry 313 (2022) 123293

Contents lists available at ScienceDirect

Journal of Solid State Chemistry

journal homepage: www.elsevier.com/locate/jssc

Densely packed Ga_2O_3 nanostructured film via pH-controlled crystal growth and memristive properties

Siddhartha Suman [a], Ajay Kumar Kushwaha [a,b,*]

[a] Department of Metallurgy Engineering and Materials Science, Indian Institute of Technology Indore, Simrol, Indore, M.P, 453552, India
[b] Centre for Advanced Electronics, Indian Institute of Technology Indore, Simrol, Indore, M.P, 453552, India

ARTICLE INFO

Keywords:
Gallium oxide
Beaker chemistry
Densely packed nanostructured films
Charge carrier density
Memristors

ABSTRACT

Gallium Oxide (Ga_2O_3) nanostructured film is deposited via a single step aqueous method by controlling the pH value of precursor solution. The uniformity, density and crystallite size varies when the pH of precursor solution changes from pH 6 to pH 9. The as-deposited nanostructured film is present in hydroxide crystalline phase which gets converted to a mixed phase ('α' and 'β') when heat treated at 600 °C. The densely packed Ga_2O_3 nanostructured film (at pH 8) shows better electrical conductivity and stable current density of 10^{-8} A/cm^2. The memristive measurement for densely packed nanostructured film results in R_{OFF}/R_{ON} ratio in order of 10^2, whereas the V_{set} and V_{reset} values are observed to be 2.7V and −3.1V respectively. This single step process is suitable for deposition of good quality, large crystallite, densely packed nanostructured Ga_2O_3 films that can be utilized in various electronic and optoelectronic applications.

1. Introduction

Gallium oxide (Ga_2O_3) is an emerging inorganic material that has shown its utility in various applications such as conventionally considered catalytic and gas sensing properties, UV sensors, electronics devices etc. [1–5]. Subsequently in the past few years, Ga_2O_3 has enthralled researchers as an emerging semiconductor material for various solid-state electronic devices [6]. Ga_2O_3 has been proposed to be a good competitor to traditional semiconducting materials like Si, SiC, GaN in power electronics [7,8]. Kura et al. fabricated chromium doped Ga_2O_3 films using co-sputtering technique for resistive memory devices where they studied the role of varying gallium to oxide ratio. $Ga_{0.82}Cr_{0.18}O_{12}$ based film was found to be the best performing switching device [9]. R.V. Tominov et al. reported memristors with a high resistance state (HRS) at +4V and a low resistance state (LRS) at -6V for gallium oxide nanostructures films fabricated via local anodic oxidation [10]. Bipolar resistive switching was reported by M.N. Almadhoun et al., using the junction between gallium oxide and p-type silicon and resistance ratio of 10^8 with retention time of 10^5 s were observed. The nanoscale layer of gallium oxide supported the gallium filament formation and dissolution, resulting in reversible switching [11]. Nanostructures of Ga_2O_3 (nanowires, nanorods, nanobelts and nanosheets) are presently gaining momentum with respect to nanoscale applications targeting evolution of better electronics and optoelectronics devices [12]. A. Paraye et al. observed increased pH and sulphur concentration resulted in a decrease in thickness when CZTS was electrodeposited on gold substrate in a single step with glycine as the complexing agent [13]. The effect of the pH of sol on the morphological and optical properties of CuO thin films prepared by the sol–gel dip coating process, showing significant improvement in the surface morphology and average grain size of films by using different pH solutions were reported by S.S. Niavol et al. Investigations with respect to synthesis and characterization of Ga_2O_3 nanostructures are making headway rapidly [14,15]. Alteration of synthesis parameters (for deposition of nanostructured films) lead to significant control over properties of Ga_2O_3 films. Ga_2O_3 is polymorphic in nature and mostly available in 'α', 'β', 'γ' and 'δ' phases. The tetrahedral 'α' phase and monoclinic 'β' phase are most stable phases and are being synthesized using various approaches [16,17]. The physical vapor deposition or vacuum based techniques have rendered very high quality of Ga_2O_3 films. These methods require high-end equipment that led to higher cost of film deposition, which may not be very suitable for several low-cost applications. Therefore, the solution-based approaches are desirable as they can be used for deposition of large area films at lower cost, with minimum usage of high-end equipments.

Y. Kokubun et al. used sol-gel method to prepare Ga_2O_3 film for ultraviolet photo detector. They prepared the precursor solution at 60 °C

* Corresponding author.Department of Metallurgy Engineering and Materials Science, Indian Institute of Technology Indore, Simrol, Indore, M.P, 453552, India.
E-mail address: akk@iiti.ac.in (A.K. Kushwaha).

https://doi.org/10.1016/j.jssc.2022.123293
Received 8 March 2022; Received in revised form 18 May 2022; Accepted 28 May 2022
Available online 6 June 2022

and performed spin coating to form the film, followed by drying at 90 °C and annealing at 300 °C [18]. Spraying of aqueous solution of gallium nitrate carried out at 300 °C by Hao et al. demonstrated good quality of Ga_2O_3 films [19]. T. Miyata et al. sprayed the mixture of gallium chloride and ethanol over a hot substrate (700 °C–800 °C) for deposition of poly crystalline β-phase gallium oxide film [20]. T. Kawaharamura et al. used the mist of gallium acetylacetonate and hydrochloric acid to deposit α-Ga_2O_3 at 400 °C [21]. A soft chemistry route without using surfactant was demonstrated to produce different morphology of gallium oxide with controlled particles size [22]. Tas et al. synthesized gallium hydroxide by adding urea to an aqueous solution of gallium nitrate at 90 °C, and Ga_2O_3 was achieved after annealing at 600 °C [23]. Nanorods of gallium oxide hydrate was grown by J. Zhang et al. using hydrothermal process by mixing gallium oxide with hydrochloric acid in DI water and heating the solution at 180 °C for 24 h. Aspect ratio of the nanorods were controlled by adding different amount of diethylene glycol [24]. Reddy et al. synthesized Ga_2O_3 nanorods via hydrothermal method, by using ammonium hydroxide as a pH balancer at 95 °C [25]. Synthesis of GaOOH nanorods via laser ablation followed by solution phases was studied by Huang et al. [26]. A study on growth of vertical array of α-GaOOH was carried by H. Lian et al. by building a continuous flow reactor and the reaction was carried at 95 °C [27]. R Gopal et al. reported cubic phase of Ga_2O_3 by using salicydeneimin modified precursor of gallium isopropoxide via sol gel synthesis method [28]. M. Yu et al. studied new approach for producing high-performance solar blind photodetectors and using sol-gel process successfully produced the α/β phase polycrystalline Ga_2O_3 thin film. The photodetector displayed high detectivity and fast reaction time post optimization of the annealing environment [29]. Li Yuan et al. investigated structural, morphological and electrical properties for solution processed Ga_2O_3 thin film and studied the role of amorphous Ga_2O_3 thin film in fabricating TFTs [30]. In most of the solution-based approach, the deposition was mostly performed at elevated temperature and was followed by multiple steps including annealing. The role of solution pH was investigated mainly to establish different morphologies and to tune various properties of metal oxide nanostructures. However, the impact of pH control in solution process growth of nanostructures in development of densely packed films, is yet to be explored.

Herein, a single step beaker chemistry approach is demonstrated to deposit the GaO(OH) nanostructured film at lower temperature followed by annealing to achieve Ga_2O_3 films. The deposition is carried out at 60 °C with single precursors in a beaker and hotplate, that makes it simple and feasible for large area deposition of Ga_2O_3 films. Notably, control over precursor pH leads to formation of large crystallites and denser Ga_2O_3 nanostructures. An optimum value of pH-8 leads to relatively denser and compact Ga_2O_3 nanostructured film when compared to other pH values. Structural analysis of thin films reveals the presence of 'α' and 'β' phases, after they are annealed at 600 °C. The gallium oxide nanostructures have diamond like morphology, with maximum absorption in the UV range pertaining to wide bandgap properties. The charge carrier density (N_D) for the Ga_2O_3 nanostructured film is in the range of $10^{17}cm^{-3}$. Memristive properties of the deposited films are investigated for deposited nanostructured film and a resistance ratio (R_{OFF}: R_{ON}) of 10^2, with set and reset voltages at 2.7V and −3.1V, respectively were observed for films annealed at 600 °C. The developed procedure is simple and is potentially beneficial for large scale deposition of Ga_2O_3 films that can be used for electronics and memory-based device applications.

2. Experimental section

2.1. pH-controlled growth/enlargement in Ga_2O_3 nanostructures toward film formation

A single step beaker chemistry was performed at 60 °C to deposit gallium hydroxide films on fluorine doped tin oxide (FTO) substrates. Prior to deposition reaction, the FTO substrate were cut into size of 2cm × 1cm followed by cleaning of the substrate to eliminate the native unwanted particles and remove carbon particles present on the surface. The cleaning process involved sonicating FTO substrates in soap solution, DI water, acetone and ethanol, respectively for 15 min each; after cleaning the substrates were blow-dried. Cleaned substrates were partially covered with the teflon tape with a hanging support. The schematic in Fig. 1 depicts the way substrates were suspended in gallium chloride ($GaCl_3$) solution. The precursor solution was prepared dissolving 0.1M $GaCl_3$ in 20ml DI water under constant stirring at room temperature. The solution was stirred for 15 min till it turned transparent. The beaker with solution was kept at preheated hot plate at 60 °C. Ammonia solution was added drop wise to the above heated solution, to attain pH values of 6, 7, 8, 9 and 10 from initial pH value of 2.1. The solution turned milky white once the pH reached 6. On subsequent addition of ammonia, the solution became relatively viscous. The cleaned FTO substrate was then hung inside the beaker to submerge substrate into the solution. After 10 h the FTO substrates were taken out and allowed to naturally cool down to room temperature. Eventually substrates were cleaned by sonicating in DI water. The cleaned substrates were dried at 70 °C for an hour. Lastly, all the thin film substrates were annealed at 600 °C for the duration of 30 min.

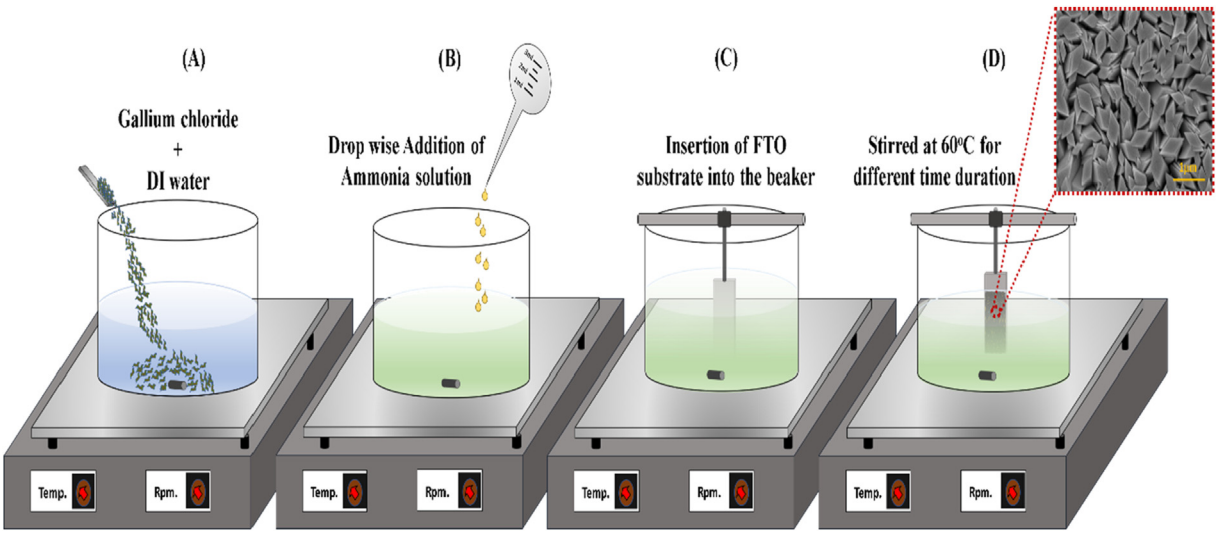

Fig. 1. Gallium oxide film deposition process via aqueous solution route by simple beaker chemistry.

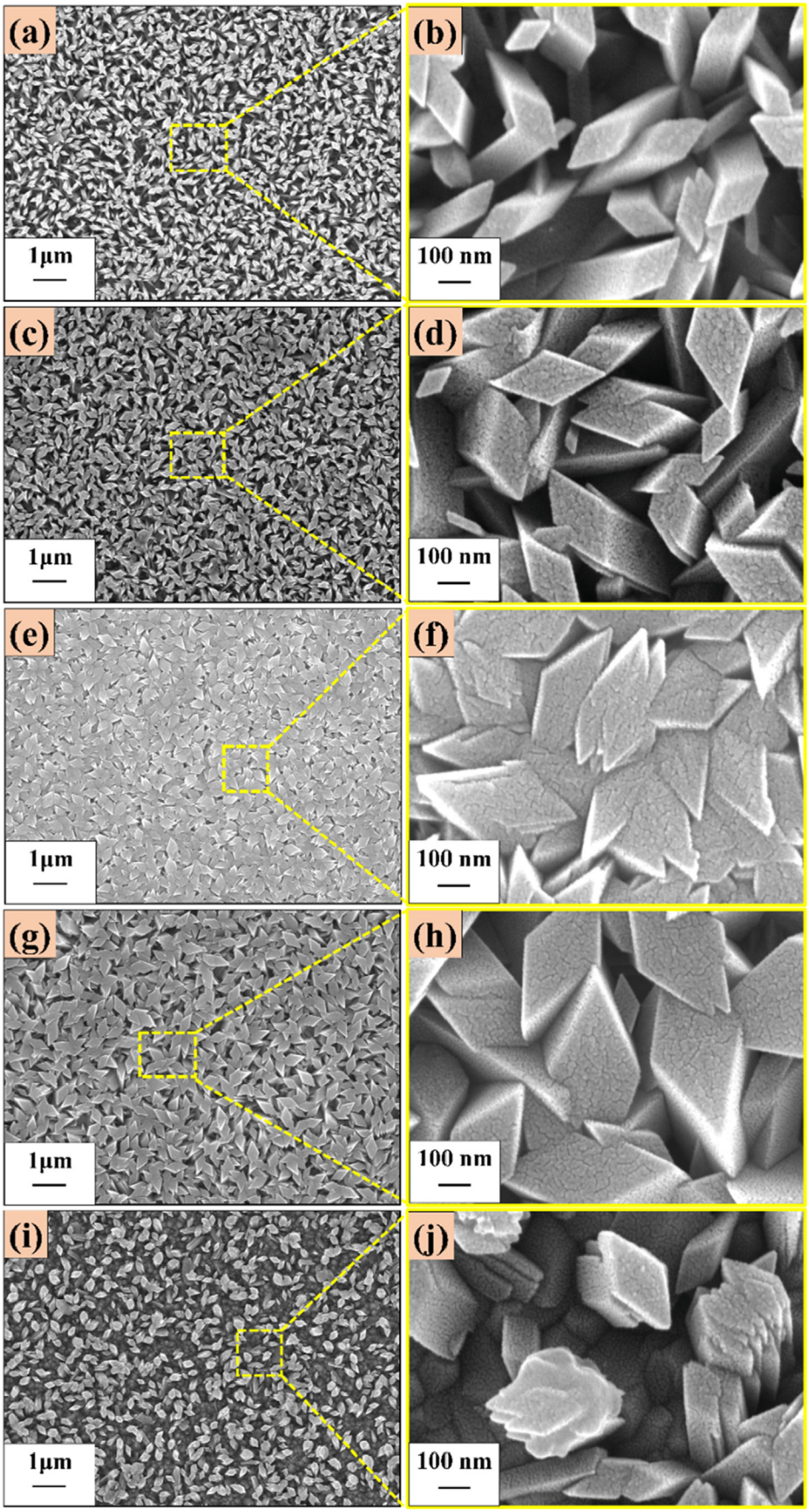

Fig. 2. Scanning electron micrograph of aqueous route deposited diamond shaped nanostructured films: (a & b) deposited at pH 6, (c & d) deposited at pH 7, (e & f) deposited at pH 8, (g & h) deposited at pH 9 and (i & j) deposited at pH 10.

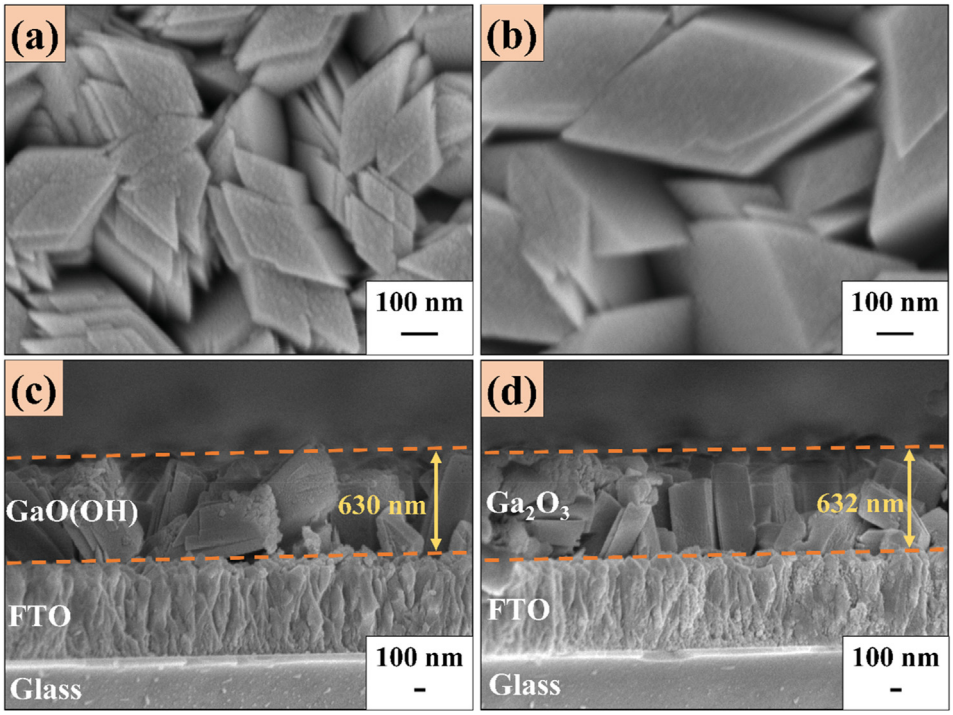

Fig. 3. Scanning electron micrograph of Ga_2O_3 nanostructured films (deposited at pH 8); (a) diamond like morphology of Ga_2O_3 nanostructure in as-deposited film, (b) annealed Ga_2O_3 nanostructured film, (c) cross section image of as-deposited film, (d) cross section image of annealed Ga_2O_3 nanostructured film.

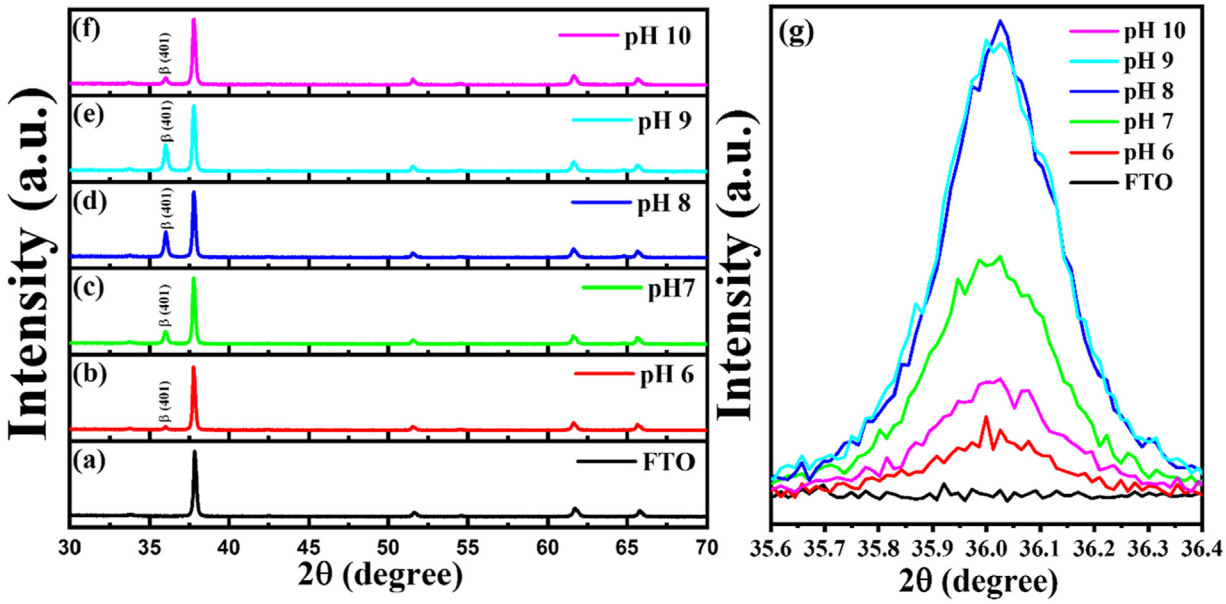

Fig. 4. XRD pattern of Ga_2O_3 nanostructured films grown at different pH (thermally annealed at 600 °C); (a) FTO substrate, (b) at pH 6, (c) at pH −7 (d) at pH 8,(e) at pH 9, (f) at pH 10 and (g) in-large XRD pattern for (401) peak.

2.2. Ga_2O_3 films characterization

The deposited Ga_2O_3 films were characterized using Bruker D-8 advance X-ray diffractometer instrument with Cu as source of X-ray with a wavelength of 1.54 Å, at room temperature. Glancing angle XRD (GIXRD) was operated with step size of 0.04° and omega for maximum intensity was 1.5° for the thin films. Morphological properties were analyzed by scanning electron microscope (JEOL make model number: JSM-7610F Plus). UV–Visible spectroscopy measurement was done by using UV–Vis instrument (Simadzu-2600). The Mott Schottky analyses were performed using an electrochemical system (Auto-Lab, PG start 204A). Three electrodes set up were used, Ga_2O_3 on FTO substrate as an anode electrode, Pt wire as cathode and Ag/AgCl electrode as reference electrode. The electrode was dipped into liquid electrolyte containing buffer solution of potassium hydroxide (KOH), 0.1M in concentration. The pH of the electrolyte was fixed at 12. I–V characteristics were measured using a source meter unit (Keithley 2604B).

3. Results and discussion

3.1. Effect of pH value of the precursor's solution on morphological and structural properties of Ga_2O_3 nanostructured films

Fig. 2(a)-(j) depicts the surface topography of the Ga_2O_3

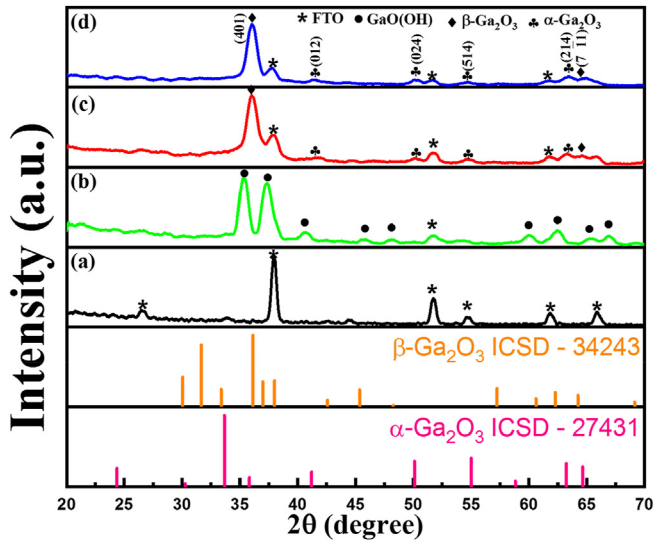

Fig. 5. XRD pattern of Ga_2O_3 nanostructured films (a) FTO substrate, (b) as-deposited film, (c) film annealed at 500 °C and (d) film annealed at 600 °C.

nanostructured films deposited at different pH (6, 7, 8, 9 and 10) of precursor solution. Formation of diamond like structure can be seen in all the nanostructures grown with different pH. As the pH of precursor solution increases to a value of pH 8, both the size of Ga_2O_3 nanostructure and the density, increases. Further increase in the pH value to 9 and 10, does not result in optimum deposition of nanostructures. In the nucleation stage, film growth begins with the nucleation of crystallites, followed by formation of grains, which coalesce to cover the entire substrate surface and exhibit a dense structure. The overall growth mechanism with schematic of Ga_2O_3 nanostructured film formation is discussed in the supplementary material (Fig. S1).

Ga_2O_3 nanostructure grown at pH 6 exhibit dimensions of approx. (210 nm × 110 nm) which increases to approx. (530 nm × 300 nm) for pH 8. On comparing nanostructures growth at pH 8 with pH 7, pH 9 and pH 10, 1.5 times crystal enlargement is observed. The uniformity of Ga_2O_3 nanostructure at pH 8 is better in comparison to the nanostructure at other pH values. The average area of the Ga_2O_3 nanostructures at pH 8 as shown in supplementary material (Fig. S2). Thus, it is inferred that Ga_2O_3 nanostructure density varies as a function of pH value. The pH of the precursor solution affects the rate of the reaction and nucleation. When ammonia is added to the solution it results in formation of NH^{4+} and OH^- ions as ammonia gets hydrolyzed. Thus, giving rise to OH^- ions concentration in the solution. Thus, a specific morphology is obtained at a set amount of OH^- ion concentration. When the pH is increased the OH^- ions concentration also increases that gives rise to the anisotropic growth direction, as a result change in morphology take place. On further increasing the pH, the growth rate gets increased due to increase of the OH^- concentration that changes the reaction rate which also results in new morphology. On increasing the concentration of OH^- ions as compared to Ga^{3+} ions concentration, reaction rate changes due to which precipitation rate is changed in the solution [31]. Secondly, the dissolution of precipitation occurs due to the interaction between Ga^{3+} ions and OH^- ions. At lower pH the large amount of Ga^{3+} is formed giving rise to formation of seed layer and therefore results in a specific morphology [32].

The surface of Ga_2O_3 nanostructure become smooth when thermally annealed at 600 °C (Fig. 3). The surface smoothening is caused due to thermal decomposition of molecules present at the surface, which might be a function of the rate of change of temperature with time [33]. Thermal annealing is also beneficial in removing structural and surface defects from the crystals [34,35]. The measured thickness of nanostructured film is approx. 630nm, (Fig. 3c and d). The EDAX analysis reveals the Ga:O atomic percentage ratio to be 31.6%: 68.4% for as-deposited films and 39.5%:60.5% for annealed films, as shown in supplementary material (Fig. S3). The concentration of gallium increases with respect to oxygen after annealing because thermal decomposition of the gallium oxyhydroxide occurs at higher temperature and removes surface hydroxyl groups [22].

Structural study for the grown nanostructured films at different pH are done using XRD analysis, as shown in Fig. 4. The diffraction peak (401) at 36.03° confirms the presence of monoclinic phase (β) of Ga_2O_3 which is known to be the most stable phase of Ga_2O_3. The XRD pattern of the FTO substrate is also evident for all the nanostructured films deposited at various pH values. Ga_2O_3 nanostructured films deposited at pH 8 and pH 9, have the intense (401) XRD peak. However, Ga_2O_3 nanostructured films deposited at pH 10 shows decrease in intensity of the (401) peak. An intense peak of (401) indicates better orientation and dense Ga_2O_3 nanostructure growth with improved crystallinity. Further, full width at half maximum (FWHM) value of (401) plane is calculated to be 0.27, 0.25, 0.22, 0.22 and 0.24 for Ga_2O_3 nanostructured films deposited at pH 6, pH 7, pH 8, pH 9 and pH 10, respectively. The full

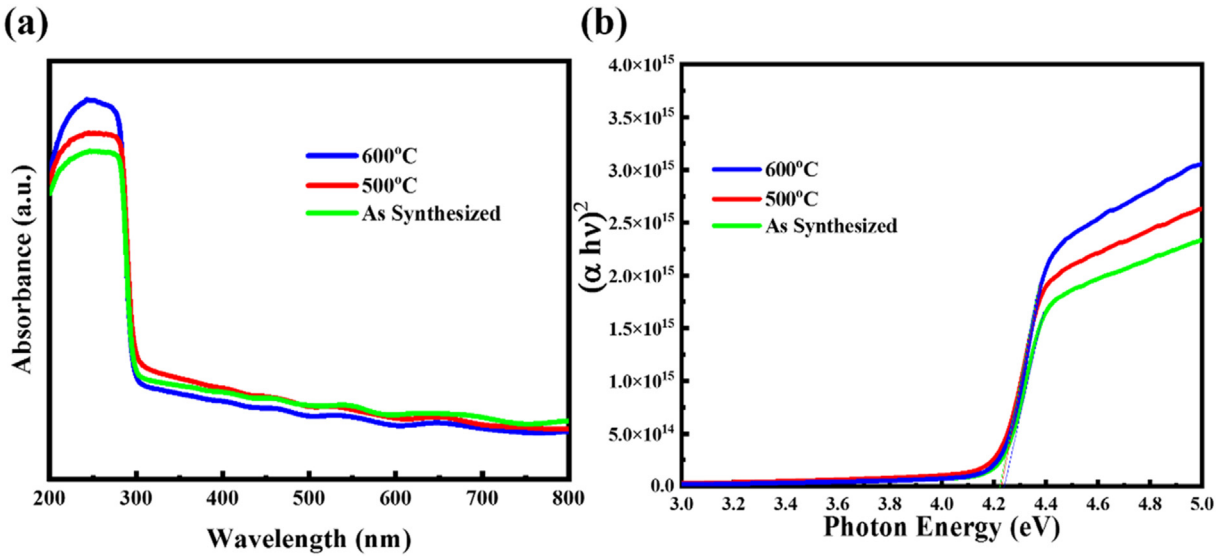

Fig. 6. UV–Visible spectra of solution processed Ga_2O_3 nanostructured film (a) absorption spectra of as-deposited films and films annealed at 500 °C and 600 °C and (b) figure depicts the tauc plot of Ga_2O_3 film.

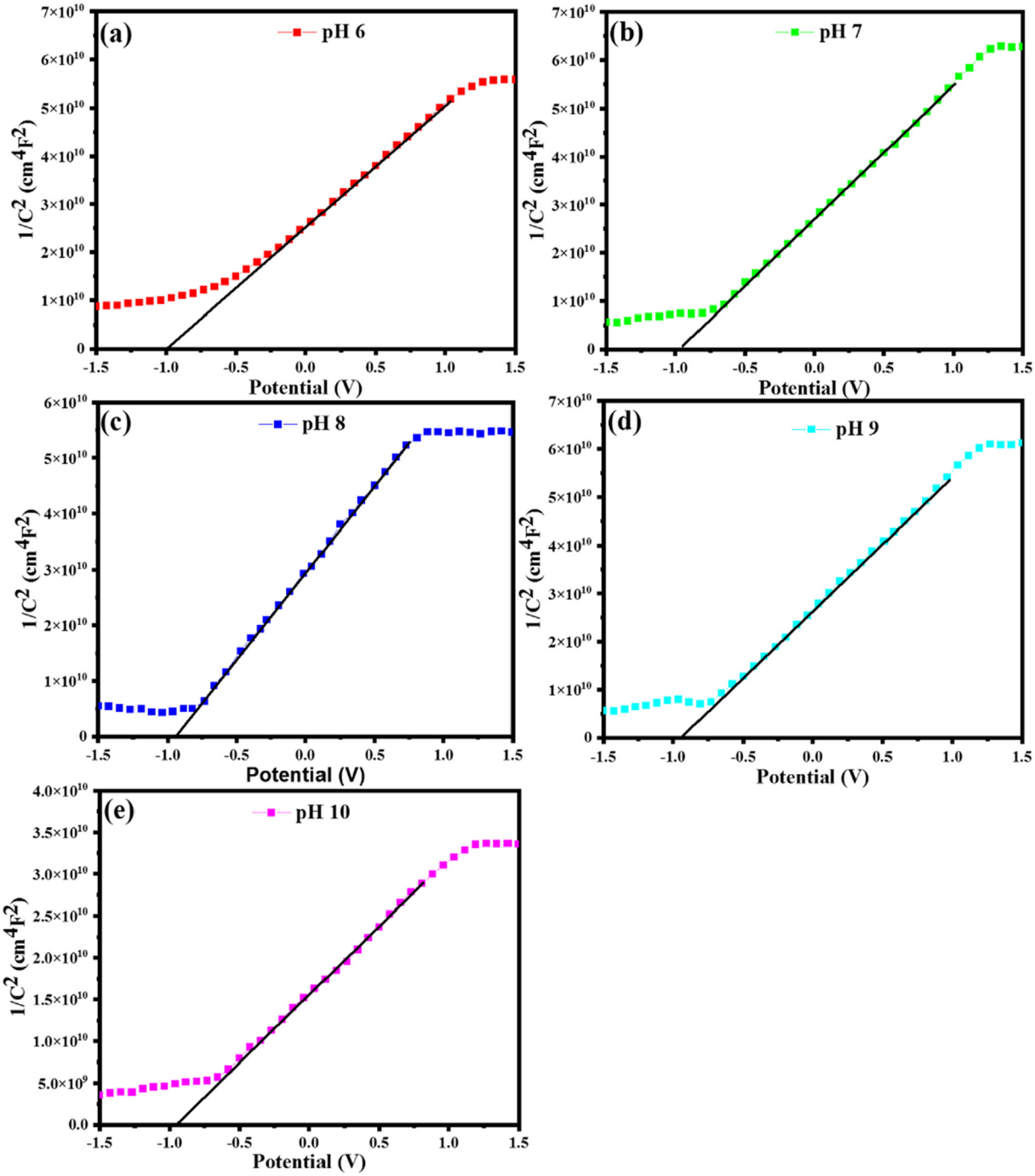

Fig. 7. Mott-Schottky plots for gallium oxide (Ga_2O_3) nanostructured film deposited at different pH; (a) obtained at pH 6, (b) obtained at pH 7, (c) obtained at pH 8, (d) obtained at pH 9 and (e) obtained at pH 10.

width at half maximum (FWHM) of the plane (401) decreases with increase in the pH value from 6 to 9. Crystallite size increases from 30.9 nm at pH 6, through 33.5 nm (pH 7), 37.9 nm (pH 8) to 38.0 nm at pH 9 but decrease to 34.7 nm for pH 10.

The effect of annealing on the structural properties of dense Ga_2O_3 nanostructured film is further investigated using glancing angle X-ray diffraction (GIXRD) patterns (Fig. 5). The as-deposited film has diffraction peaks of (210), (111), (211), (311), (410), (511), (020), (610) and (121) at 2 theta value of 35.29°, 37.25°, 40.5°, 45.7°, 48.07°, 60.1°, 62.44°, 65.32° and 66.91°, respectively which indicate formation of gallium oxyhydroxide phase. When films are annealed at 500 °C and 600 °C, the XRD pattern get changed and diffraction peaks of (401), (012), (024), (511), (214) and (71–1) appears at 36.03°, 41.35°, 50.19°, 54.73°, 63.48° and 64.94° which corresponds to 'α' and 'β' phase of Ga_2O_3. The reflections of the annealed sample were indexed according to the β-Ga_2O_3 ICSD structure 34243 (JCPDS PDF no. 01-076-0573, monoclinic phase) [36] and reflection pattern of α-Ga_2O_3 was according to JCPDS PDF no. 00-006-0503. Presence of 'β' phase can be confirmed by the appearance of (401) and (71–1) planes in both films annealed at 500 °C and 600 °C. Due to FTO substrate, further increase in annealing temperature is not possible, which may offer a pure 'β' phase [37].

Fig. 6(a) shows the UV–Vis absorption spectra of the Ga_2O_3 nanostructured films. The Ga_2O_3 film exhibit maximum absorption intensity around 235 nm (UV–C) in deep UV region for both as-deposited and

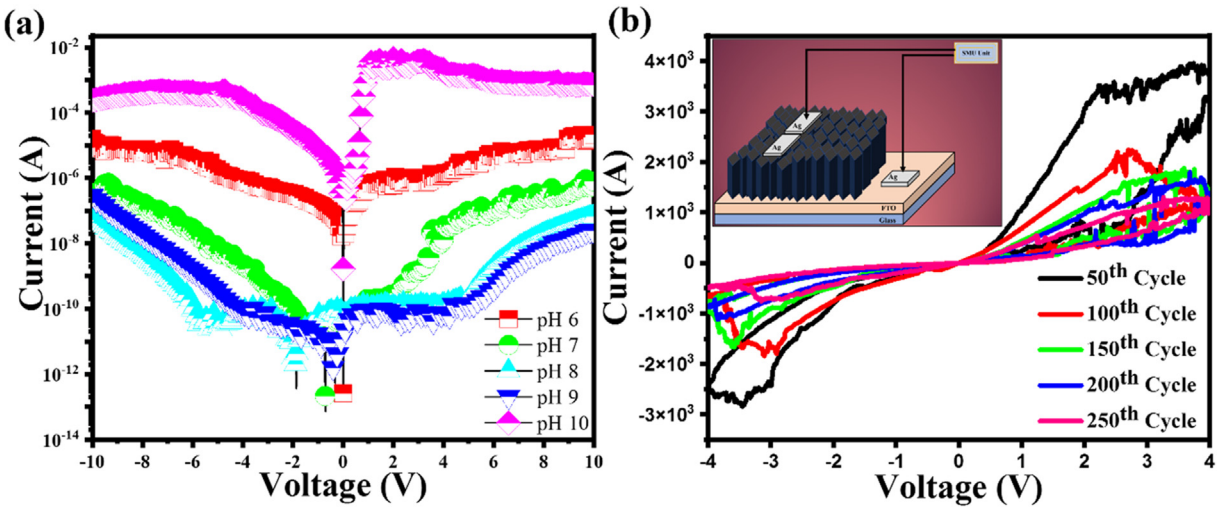

Fig. 8. (a) Current-Voltage characteristics of the different pH-based films and (b) memristive behavior of the densely packed Ga_2O_3 nanostructured film representing, individual cycles for memristive behavior (i.e. 50th Cycle, 100th Cycle, 150th Cycle, 200th Cycle and 250th Cycle).

annealed films. Since the absorption is negligible in visible range therefore the Ga_2O_3 is transparent in nature which does not reflect any color from the visible range. The optical bandgaps for the films were calculated from the UV–Vis data using power law for direct bandgap semiconductors [38,39]. The optical absorption coefficients were estimated. The bandgap is calculated to be 4.14eV for as-deposited films, 4.20eV and 4.24eV for film annealed at 500 °C and 600 °C, respectively (Fig. 6(b)).

3.2. Electrical and memristive properties of Ga_2O_3 nanostructured films

The electrolyte/electrode interface is examined to calculate the charge carrier density and the flat band potential of Ga_2O_3 films. The Mott-Schottky plot of Ga_2O_3 film is shown in Fig. 7(a–e). The charge carrier density of the Ga_2O_3 film deposited at pH 6, pH 7, pH 8, pH 9 and pH 10 are 4.7×10^{17}, 4.1×10^{17}, 3.3×10^{17}, 3.7×10^{17} and 4.1×10^{17}, respectively. The flat band potential for these films deposited at different pH is found to

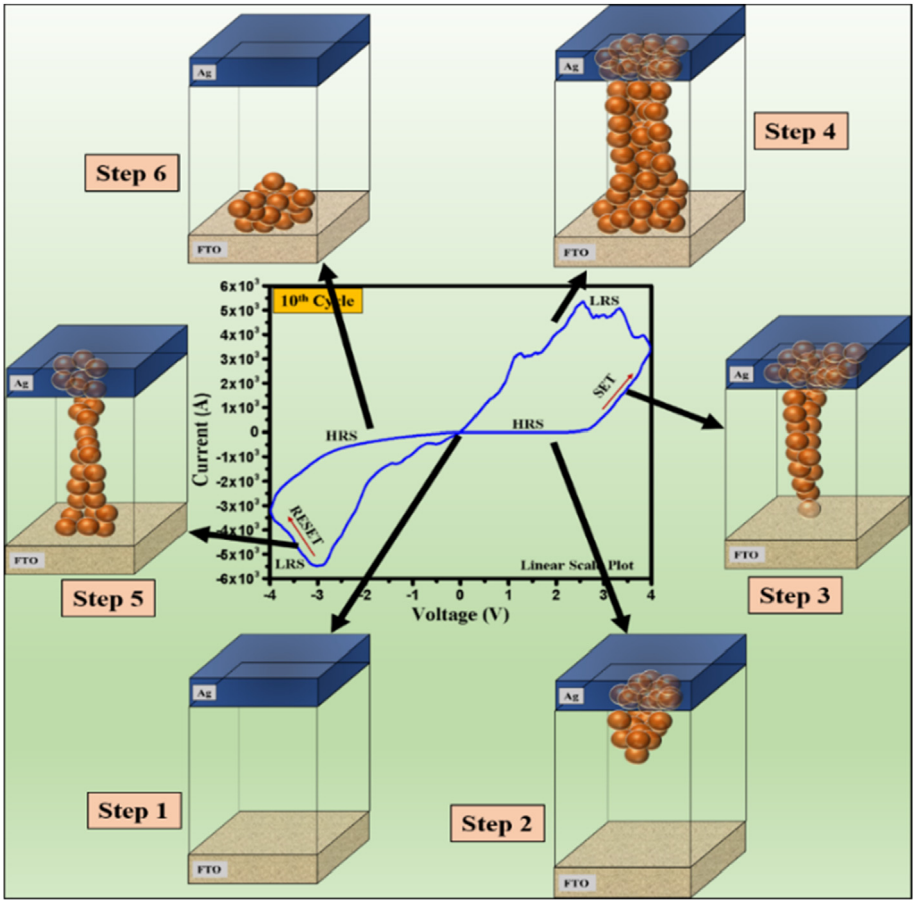

Fig. 9. Mechanism for the Ga_2O_3 nanostructured film grown on FTO substrate showing memristive behavior.

be in the range of −0.90V to −0.99V. It has been reported that the carrier concentration of epitaxial layer Ga_2O_3 is in the range of 10^{15} to $10^{17}cm^{-3}$ [40]. Films produced via aqueous route also have charge carrier density in similar range, hence these films can be considered suitable for the electronic device applications. The cyclic voltammetry measurements of Ga_2O_3 nanostructure as working electrode shows the reduction peak at −0.96V as mentioned in supplementary material (Fig. S4).

The Ga_2O_3 nanostructured films grown at different pH are further investigated by performing current voltage measurements. The Ga_2O_3 nanostructured films deposited at pH 6, 7 and 10 show general current characteristics while Ga_2O_3 nanostructured films deposited at pH 8 and pH 9 show a gradual and slow change in current value. This observation indicates that the charge passing through the relatively dense films (for pH 8 and pH 9) encounter more resistance. Whereas, for Ga_2O_3 nanostructured films at pH 6, pH 7 and pH 10 the movement of charge is partially supported by FTO substrate and leading to high conductivity. Hence, the densely packed nanostructured films show better characteristic of a Ga_2O_3 nanostructured film and relatively suitable structure for various applications like optoelectronic devices, memory devices etc.

The Ga_2O_3 nanostructured films deposited at pH 8 are tested for memristive behavior. The nanostructured films of as deposited and annealed films at 500 °C have not shown a good response for memristive system as mentioned in supplementary material (Figs. S5(a and b)). Film annealed at 600 °C showed interesting results. Fig. 8(b) shows typical characteristic curve of memristors. For better visualization of the memristive cycle individual cycles are shown in supplementary material (Figs. S6(b–e)). The basic structure of the device is given in inset of Fig. 8(b) where a top contact of silver is deposited on the nanostructure film of Ga_2O_3, whereas a bottom contact is of FTO/Ag made on surface of substrate, replicating a metal insulator metal (MIM) structure. Herein silver is the metal contacts and gallium oxide is the sandwiched insulator. The Ga_2O_3 based memristive device is subjected to a potential window of -4V to +4V. A high resistance state (HRS) is maintained until the applied voltage reaches 2.7V (V_{set}). Further increase in voltage leads to sudden jump in current attaining SET stage. When the applied voltage is reversed, the current stays the same, maintaining a low resistance state (LRS). The low resistance state continues for some time. On applying negative bias, similar phenomenon is observed. At −3.1V (V_{RESET}) the reset is triggered, and the device attains RESET stage. Further change in voltage conditions the device to enter high resistance state (HRS) again. The resistance ratio (R_{OFF}: R_{ON}) is in the order of 10^2 which proposes that the information can be stored with significant difference and can be recalled after some time duration. The device was tested for 250 cycles as shown in supplementary material (Fig. S6 (a)). Some recent work reported for gallium oxide based memristors have resistance ratio from 2 to 20 (at 0.7V) for co-sputtered gallium oxide and chromium based devices [9]. In other work Ga_2O_3 nanostructures were incorporated as the resistive material for memristor in which +4V and -6V were the potentials where HRS and LRS were triggered respectively, resistance ratio was evaluated to 5 for the device [10]. Device based on bipolar resistive switching mechanism reported a resistance ratio of 10^8 for gallium oxide and p-type silicon based device, the HRS and LRS were trigger at +2.5V and -2V, respectively [11]. The result shows that the nanostructure of Ga_2O_3 films can be casted for memory devices and can be utilized for neuromorphic applications.

The overall mechanism of storing charge can be understood from Fig. 9. At 0 V the device is in reset state or initial state where no interaction between ions is taking place. When voltage is increased, the ions start to move through the semiconductor as shown in step 2. However, this potential is not enough to make a proper channel for the flow of charges thus the device is in high resistance state. Once the potential is increased, the channel formation takes place and a sudden change in current value at a potential is achieved in step 3. In step 4, the channel becomes prominent because of large value of current due to full migration of Ag^+ ions into the semiconductor, making a direct path from top to bottom contacts. On applying the negative potential or even after removal of potential, the current value remains same. Top contact undergoes oxidation at surface, resulting in changes in chemical state of the deposited metal, which might affect the charge trapping of metal contact. Charge carrier trapping occurs due to the movement of charges from delocalized states to localized state of Ga_2O_3, and trapped states can be in the crystal lattice of Ga_2O_3 intrinsic to the possible ligand on the nanocrystal interface or within the whole environment. This phenomenon is illustrated as the memristive behavior of the device. In the step 5, the channel tends to decrease, and the migrated ions tend to reduce the channel length of the device. This is followed by step 6 where the channel is broken; the migrated ions return to the top contact leaving behind some ions near the bottom contact which will help the device for faster switching by making the filament formation fast in the next cycle. As there is no flow of electrons taking place in the device, it tends to get back to high resistance state or reset state.

4. Conclusion

Densely packed Ga_2O_3 nanostructured films were synthesized using single step low temperature chemical growth process. Variation in the topography of nanostructured film was a result of different pH value. Annealing of the film caused phase change leading to a stable phase of Ga_2O_3. Ga_2O_3 nanostructured films deposited at pH 8 were relatively denser as compared to pH 6, pH 7, pH 9 and pH 10. The UV–Vis spectroscopy showed effective absorption in the short UV range making Ga_2O_3 nanostructured thin films a suitable candidate for solar blind photodetector and UV sensors. The Ga_2O_3 nanostructured film have charge carrier concentration in the range 10^{17} cm^{-3} signifying their utility for high-power based electronics devices. I–V characteristics curve showed a uniform current density value for pH 8 and pH 9 as compared to pH 6, pH 7 and pH 10. Memristor device was fabricated using Ga_2O_3 nanostructured film deposited at pH 8, with resistance ratio of 10^2 and. set and reset voltages of 2.7V and −3.1V respectively. Low temperature based Ga_2O_3 film formation over FTO substrate was found to be aptly suitable method for various applications in the field of optoelectronics, electronics devices, sensors, coating etc.

CRediT authorship contribution statement

Siddhartha Suman: Conceptualization, Methodology, Validation, Investigation, Data curation, Formal analysis, Writing – original draft, Writing – review & editing, Visualization. **Ajay Kumar Kushwaha:** Conceptualization, Methodology, Validation, Writing – review & editing, Supervision, Project administration, Resources, Funding acquisition.

Declaration of competing interest

The authors declare that they have no competing financial interests or personal relationships that could have appeared to influence the work reported in this paper.

Acknowledgment

We acknowledge the financial support by ECRA-SERB, New Delhi, in the form of a project (Grant no. - ECR/2017/000682) and DST, India (Grant no. - DST/INSPIRE/04/2015/002498). The experimental facilities were provided by IIT Indore. The authors gratefully acknowledge the Department of Metallurgy Engineering and Materials Science to provide the FE-SEM and XRD facility.

Appendix A. Supplementary data

Supplementary data to this article can be found online at https://doi.org/10.1016/j.jssc.2022.123293.

References

[1] C.H. Liang, G.W. Meng, G.Z. Wang, Y.W. Wang, L.D. Zhang, S.Y. Zhang, Catalytic synthesis and photoluminescence of β-Ga_2O_3 nanowires, Appl. Phys. Lett. 78 (2001) 3202–3204, https://doi.org/10.1063/1.1374498.

[2] K.I. Shimizu, M. Takamatsu, K. Nishi, H. Yoshida, A. Satsuma, T. Hattori, Influence of local structure on the catalytic activity of gallium oxide for the selective reduction of NO by CH_4, Chem. Commun. 3 (1996) 1827–1828, https://doi.org/10.1039/cc9960001827.

[3] S. Jung, S. Jang, K.H. Baik, Ga_2O_3-based Gas Sensors, Elsevier Inc., 2018, https://doi.org/10.1016/b978-0-12-814521-0.00019-1.

[4] Gallium Oxide Thin Films, A new material for high-temperature oxygen sensors, Sensor. Actuator. B Chem. 4 (1991) 437–441, https://doi.org/10.1016/0925-4005(91)80148-D.

[5] M. Ogita, N. Saika, Y. Nakanishi, Y. Hatanaka, Ga_2O_3 thin films for high-temperature gas sensors, Appl. Surf. Sci. 142 (1999) 188–191, https://doi.org/10.1016/S0169-4332(98)00714-4.

[6] S.J. Pearton, F. Ren, M. Tadjer, J. Kim, Perspective: Ga_2O_3 for ultra-high power rectifiers and MOSFETS, J. Appl. Phys. 124 (2018), 220901, https://doi.org/10.1063/1.5062841.

[7] M. Dasog, L.F. Smith, T.K. Purkait, J.G.C. Veinot, Low temperature synthesis of silicon carbide nanomaterials using a solid-state method, Chem. Commun. 49 (2013) 7004–7006, https://doi.org/10.1039/c3cc43625j.

[8] H. Amano, Y. Baines, E. Beam, M. Borga, T. Bouchet, R. Chu, C. De Santi, M.M. De Souza, The 2018 GaN power electronics roadmap - IOPscience, J. Phys. D Appl. Phys. 51 (2018), 163001. https://iopscience.iop.org/article/10.1088/1361-6463/aaaf9d.

[9] C. Kura, Y. Aoki, E. Tsuji, H. Habazaki, M. Martin, Fabrication of a resistive switching gallium oxide thin film with a tailored gallium valence state and oxygen deficiency by rf cosputtering process, RSC Adv. 6 (2016) 8964–8970, https://doi.org/10.1039/c5ra21160c.

[10] R.V. Tominov, N.A. Polupanov, V.I. Avilov, M.S. Solodovnik, N.V. Parshina, V.A. Smirnov, O.A. Ageev, Investigation of resistive switching in gallium oxide nanostructures formed by local anodic oxidation, J. Phys. Conf. Ser. 1410 (2019), 012233, https://doi.org/10.1088/1742-6596/1410/1/012233.

[11] M.N. Almadhoun, M. Speckbacher, B.C. Olsen, E.J. Luber, S.Y. Sayed, M. Tornow, J.M. Buriak, Bipolar resistive switching in junctions of gallium oxide and p-type silicon, Nano Lett. 21 (2021) 2666–2674, https://doi.org/10.1021/acs.nanolett.1c00539.

[12] Z.R. Dai, Z.W. Pan, Z.L. Wang, Gallium oxide nanoribbons and nanosheets, J. Phys. Chem. B 106 (2002) 902–904, https://doi.org/10.1021/jp013228x.

[13] A. Paraye, R. Sani, M. Ramachandran, N.V. Selvam, Effect of pH and sulfur precursor concentration on electrochemically deposited CZTS thin films using glycine as the complexing agent, Appl. Surf. Sci. 435 (2018) 1249–1256, https://doi.org/10.1016/j.apsusc.2017.11.210.

[14] W.J.L.F.K. Shan, G.X. Liu, Structural , electrical , and optical properties of transparent gallium oxide thin films grown by plasma-enhanced atomic layer deposition, J. Appl. Phys. 98 (2005), 023504, https://doi.org/10.1063/1.1980535.

[15] Jie Wang, Huizhao Zhuang, Xiaokai Zhang, Shiying Zhang, Junlin Li, Synthesis and properties of, β-Ga_2O_3 nanostructures 85 (2018) 802–805, https://doi.org/10.1016/j.vacuum.2010.12.001.

[16] S.I. Stepanov, V.I. Nikolaev, V.E. Bougrov, A.E. Romanov, Gallium oxide: properties and applications - a review, Rev. Adv. Mater. Sci. 44 (2016) 63–86. https://www.ipme.ru/e-journals/RAMS/no_14416/06_14416_stepanov.pdf.

[17] M. Higashiwaki, K. Sasaki, H. Murakami, Y. Kumagai, A. Koukitu, A. Kuramata, T. Masui, S. Yamakoshi, Recent progress in Ga_2O_3 power devices, Semicond. Sci. Technol. (2016), 034001, https://doi.org/10.1088/0268-1242/31/3/034001.

[18] Y. Kokubun, K. Miura, F. Endo, S. Nakagomi, Sol-gel prepared B-Ga_2O_3 thin films for ultraviolet photodetectors, Appl. Phys. Lett. 90 (2007), 031912, https://doi.org/10.1063/1.2432946.

[19] J. Hao, Z. Lou, I. Renaud, M. Cocivera, Electroluminescence of europium-doped gallium oxide thin films, Thin Solid Films 467 (2004) 182–185, https://doi.org/10.1016/j.tsf.2004.03.037.

[20] T. Miyata, T. Nakatani, T. Minami, Manganese-activated gallium oxide electroluminescent phosphor thin films prepared using various deposition methods, Thin Solid Films 373 (2000) 145–149, https://doi.org/10.1016/S0040-6090(00)01123-8.

[21] T. Kawaharamura, G.T. Dang, M. Furuta, Successful growth of conductive highly crystalline Sn-doped α-Ga_2O_3 thin films by fine-channel mist chemical vapor deposition, Jpn. J. Appl. Phys. 51 (2012), 040207, https://doi.org/10.1143/JJAP.51.040207.

[22] Y. Zhao, R.L. Frost, J. Yang, W.N. Martens, Size and morphology control of gallium oxide hydroxide GaO(OH), nano- to micro-sized particles by soft-chemistry route without surfactant, J. Phys. Chem. C 112 (2008) 3568–3579, https://doi.org/10.1021/jp710545p.

[23] A.C. Taş, P.J. Majewski, F. Aldinger, Synthesis of gallium oxide hydroxide crystals in aqueous solutions with or without urea and their calcination behavior, J. Am. Ceram. Soc. 85 (2002) 1421–1429, https://doi.org/10.1111/j.1151-2916.2002.tb00291.x.

[24] J. Zhang, Z. Liu, C. Lin, J. Lin, A simple method to synthesize β-Ga_2O_3 nanorods and their photoluminescence properties, J. Cryst. Growth (2005) 99–106, https://doi.org/10.1016/j.jcrysgro.2005.02.060.

[25] L.S. Reddy, Y.H. Ko, J.S. Yu, Hydrothermal synthesis and photocatalytic property of β-Ga_2O_3 nanorods, Nanoscale Res. Lett. 10 (2015) 364, https://doi.org/10.1186/s11671-015-1070-5.

[26] C.C. Huang, C.S. Yeh, GaOOH, and β- and γ-Ga_2O_3 nanowires: preparation and photoluminescence, New J. Chem. 34 (2010) 103–107, https://doi.org/10.1039/b9nj00392d.

[27] H. Liang, F. Meng, B.K. Lamb, Q. Ding, L. Li, Z. Wang, S. Jin, Solution growth of screw dislocation driven α-GaOOH nanorod arrays and their conversion to porous $ZnGa_2O_4$ nanotubes, Chem. Mater. 29 (2017) 7278–7287, https://doi.org/10.1021/acs.chemmater.7b01930.

[28] R. Gopal, A. Goyal, A. Saini, M. Nagar, N. Sharma, D.K. Gupta, V. Dhayal, Sol- gel synthesis of Ga_2O_3 nanorods and effect of precursor chemistry on their structural and morphological properties, Ceram. Int. 44 (2018) 19099–19105, https://doi.org/10.1016/j.ceramint.2018.07.173.

[29] M. Yu, C. Lv, J. Yu, Y. Shen, L. Yuan, J. Hu, S. Zhang, H. Cheng, Y. Zhang, R. Jia, High-performance photodetector based on sol–gel epitaxially grown α/β Ga_2O_3 thin films, Mater. Today Commun. 25 (2020), 101532, https://doi.org/10.1016/j.mtcomm.2020.101532.

[30] L. Yuan, S. Li, G. Song, X. wen Sun, X. Zhang, Solution-processed amorphous gallium oxide gate dielectric for low-voltage operation oxide thin film transistors, J. Mater. Sci. Mater. Electron. 32 (2021) 8347–8353, https://doi.org/10.1007/s10854-021-05408-5.

[31] G. Amin, M.H. Asif, A. Zainelabdin, S. Zaman, O. Nur, M. Willander, Influence of pH, precursor concentration, growth time, and temperature on the morphology of ZnO nanostructures grown by the hydrothermal method, J. Nanomater. 2011 (2011) 1–9, https://doi.org/10.1155/2011/269692.

[32] D. Vernardou, G. Kenanakis, S. Couris, E. Koudoumas, E. Kymakis, N. Katsarakis, pH effect on the morphology of ZnO nanostructures grown with aqueous chemical growth, Thin Solid Films 515 (2007) 8764–8767, https://doi.org/10.1016/j.tsf.2007.03.108.

[33] S. Suman, N. Mukurala, A.K. Kushwaha, Annealing induced surface restructuring in hydrothermally synthesized gallium oxide nano-cuboids, J. Cryst. Growth 554 (2021), 125946, https://doi.org/10.1016/j.jcrysgro.2020.125946.

[34] H.K.B.W.D. Kingery, Introduction to Ceramics, second ed., John Wiley & Sons, New York, 1976.

[35] L.J.P. Jolivet, M. Henry, Metal Oxide Chemistry and Synthesis, John Wiley & Sons, Chichester, 2000.

[36] R. O'Donoghue, J. Rechmann, M. Aghaee, D. Rogalla, H.W. Becker, M. Creatore, A.D. Wieck, A. Devi, Low temperature growth of gallium oxide thin films via plasma enhanced atomic layer deposition, Dalton Trans. 46 (2017) 16551–16561, https://doi.org/10.1039/c7dt03427j.

[37] A.L. Patterson, The scherrer formula for X-ray particle size determination, Phys. Rev. 56 (1939) 978–982, https://doi.org/10.1103/PhysRev.56.978.

[38] S.S. Kumar, E.J. Rubio, M. Noor-A-Alam, G. Martinez, S. Manandhar, V. Shutthanandan, S. Thevuthasan, C.V. Ramana, Structure, morphology, and optical properties of amorphous and nanocrystalline gallium oxide thin films, J. Phys. Chem. C 117 (2013) 4194–4200, https://doi.org/10.1021/jp311300e.

[39] S.K. Gullapalli, R.S. Vemuri, C.V. Ramana, Structural transformation induced changes in the optical properties of nanocrystalline tungsten oxide thin films, Appl. Phys. Lett. 96 (2010), 171903, https://doi.org/10.1063/1.3421540.

[40] A.T. Neal, S. Mou, R. Lopez, J.V. Li, D.B. Thomson, K.D. Chabak, G.H. Jessen, Incomplete ionization of a 110 meV unintentional donor in β-Ga_2O_3 and its effect on power devices, Sci. Rep. 7 (2017) 1–7, https://doi.org/10.1038/s41598-017-13656-x.